Research on Engineering Structures & Materials
www.jresm.org
MIM Research Group

Research Article

Strengthening and repairing of RC slabs using partial fiber reinforced cementitious matrix (FRCM) technique

Ali A. Abdulridha [*1,2,a], Majid M.A. Kadhima [1,b]

[1]*Department of Civil Engineering, University of Babylon, Hilla, Iraq*
[2]*Department of Civil Engineering, University of Warith Al-anbiya'a, Karbala, Iraq*

Article Info

Article History:

Received 31 Jan 2026
Accepted 20 Mar 2026

Keywords:

Carbon fiber-reinforced cementitious matrix;
Reinforced concrete slabs;
Flexural performance;
Damage repair;
Retrofitting

Abstract

Effective strengthening and repair techniques are required to extend the service life of reinforced concrete (RC) slabs affected by ageing, increased loads, and flexural deficiencies. Among modern solutions, fiber-reinforced cementitious matrix (FRCM) systems have shown effectiveness. Nevertheless, the experimental knowledge regarding the effectiveness of partial FRCM configurations on two-way RC slabs in terms of load distribution, stiffness and the ability to control crack propagation is still limited. The objective of this study is to experimentally assess the structural behavior of two-way RC slabs reinforced and repaired with different carbon-based FRCM partial layouts. A flexural loading experimental program was performed on four control and retrofitted slabs with various FRCM layouts in the tension zones. The outcomes showed that the FRCM could be applied both in strengthening and repair, which can significantly enhance load capacity, stiffness, cracking behavior and service performance compared to the control slab. FRCM layers are more efficient when directly applied over the maximum moment zone of the slabs. Consequently, this results in higher failure loads, increased stiffness and improved crack control. In general, the results demonstrate that partial application of carbon-based FRCM can be an effective and reliable solution for strengthening two-way RC slabs in the flexure zone.

1. Background

Repairing and strengthening concrete structures has been considered one of the most important issues in recent decades because these structures deteriorate over time and must conform to the most recent design guidelines [1-3].The primary objective of using strengthening and repair methods for structural members is to restore the load-bearing capacity of these elements, extend the building's lifespan, and improve its overall structural performance, whether to address existing damage or to meet new requirements, such as changing the building's function or responding to natural disasters [4, 5].

Many structural retrofitting methods, such as the RC layer technique, externally bonded steel plates, and steel jacketing, have been adopted in the construction industry. For example, Aykac, Kalkan [6] investigated the effectiveness of adding a new RC layer to a damaged slab, and they found that the ultimate load does not significantly change with this technique. Sahranavard, Jahangir [1] investigated how external ponded steel plates may enhance the flexural behavior of two-way reinforced concrete (RC) slabs. They discovered a difference in the influence of these plates on the reaction of these slabs. Aldhafairi, Hassan [7] investigated steel jacketing to improve RC beams at various temperature levels; they discovered that steel plate jacketing had no significant effect on beams at high temperatures. Although the conventional retrofitting methods

*Corresponding author: eng957.ali.abadulrazzaq@student.uobabylon.edu.iq
[a]orcid.org/ 0009-0005-4908-3737, [b]orcid.org/0000-0003-2464-0048
DOI: http://dx.doi.org/10.17515/resm2026-1489me0131rs

have assisted in the improvement of the capabilities of structural components, many researchers have indicated that these methods have serious issues, such as high temperature resisting, debonding and shear peeling [8, 9]. Thus, to overcome this drawback of these traditional technique's researchers examined the advantages of using polymer fibers as a means of reinforcement and repair for structural elements.

Fiber-reinforced polymers (FRP), as one of the least damaging rehabilitation methods, are widely used in contributing to the strengthening and repair of the building members because of their advantages, including high ductility, low self-weight and corrosion resistance [10, 11] Several common FRP materials are available, including glass FRP (GFRP), carbon FRP (CFRP), aramid FRP (AFRP), and basalt FRP (BFRP). Many forms of FRP can be used in the construction industry, such as rods, laminates, dry fibers or sheets that are bonded with the concrete by using adhesive materials [12, 13]. These techniques have become more important in the building industry in recent decades. Fang, Xu [14] investigated the effect of using carbon fiber reinforced polymer (CFRP) on the structural behavior of reinforced concrete (RC) slabs. The findings of this investigation revealed that the use of CFRP improves the flexural behavior of the RC slabs. On the other hand, the influence of basalt FRB on the flexural performance of one-way RC slabs had been studied by Erfan, Abd Elnaby [15]. Their results show an increase in the ultimate flexural strength due to the Contribution of the basalt FRB in the flexural behavior. He, Wang [16] proved by their study that the use of FRB on the RC slabs has a good influence on the structural behavior, such as cracking load and flexural stiffness. However, these methods encountered a lot of problems because of the many properties of fiber-reinforced polymers in the rehabilitation of concrete components, such as brittle behavior [17]. FRP has not been proven to outlast traditional materials for long-term service life, especially for structures that are exposed to moisture and humidity [18]. In addition, high temperatures and UV rays have a significant influence on FRP, causing their performance to decline [19, 20]. Due to these disadvantages, Fabric-Reinforced Cementitious Matrix (FRCM) appears, in some cases, more appropriate and viable, in particular in high-temperature environments as well as in more extreme environmental conditions.

Fabric-Reinforced Cementitious Matrix (FRCM) is a novel class of composite materials used for strengthening and repairing concrete structures and existing building elements that exhibit limited tensile strength, heat resistance, and/or resistance to aggressive environmental influences [21-23]. FRCM (or textile-reinforced mortar (TRM)) is an inorganic composite material in which a network of fibers, such as Poly-p-phenylenebenzobisoxazole (PBO), carbon, basalt and glass fibers are embedded within a cement matrix or cement mortar instead of organic resins or plastics [24, 25]. This provides heat, environment, and corrosion resistance advantages for the system, as well as compatibility with the existing concrete structure. Many studies try to study the impact of retrofitting the RC members with the FRCM technique [25-27]. The effect of carbon FRCM on the structural behavior of two-way RC slabs had been investigated by Kadhim, Jawdhari [23]. It can be found from their findings that the use of the FRCM system significantly enhances the ultimate load of the RC slabs. Varma, Sarker [26] considered FRP and FRCM systems at high temperatures that confine reinforced concrete cylinders. The observation suggested that the effectiveness of the FRCM system in maintaining a load-bearing system was significantly greater than that of an equivalent FRP system at elevated temperatures. Recent evaluation between FRCM versus FRP systems available in the construction industry reveals that FRCM provide better bond behavior [11, 28], presents lower dependence of bond behavior from environmental factors [27] and has better durability in temperature fluctuations and provides adhesion properties over time [29, 30].

The above literature review has shown that FRCM has high credibility and application in the rehabilitation and retrofitting of concrete members. However, a handful of studies have investigated the application of FRCM on RC slabs. The current study aims to utilize FRCM for retrofitting reinforced concrete slabs and investigate the variables that affect the performance of slabs enhanced with FRCM.

2. Experimental Program

2.1. Materials

2.1.1 Cementitious Mortar

Cementitious mortar is one of the main elements of concrete members' retrofitting [31]. In this experimental study, the cementitious mortar used to bind the materials is a commercial ready-mix cementitious binder known as Sika MonoTop®-612. The mortar is considered a single-component, polymer-modified, fiber-reinforced cementitious material. The selected mortar is designed to retrofit structural elements and is characterized by high adhesion, high final strength, sulphate resistance, significant resistance to shrinkage, and resistance to environmental factors. Sika MonoTop®-612 follows the main requirements of EN 1504-3, R3 classification and its properties are highlighted in Table 1. Although precise material-level tests (e.g., tensile, flexural, and bond compatibility) were not conducted in this macroscopic study, the manufacturer's certified parameters were adopted as a reliable baseline for structural verification.

Table 1. Properties of Sika MonoTop®-612

Property	Description
Composition	Polymer-containing cementitious mortar with different additives and synthetic fiber.
Appearance / Colour	Grey powder
Maximum grain size	Dmax: 2.0 mm
Compressive strength	28 days (ASTM C109) ~40 MPa *Testing cubes 50 x 50 x 50 mm
Mixing ratio	3 - 3.25 L of water per 25 kg bag
Fresh mortar density	Fresh mortar density 1.95 kg/L at +20 °C
Layer thickness	Min. 5 mm, Max. 30 mm

2.1.2 Fabric-Reinforced Cementitious Matrix (FRCM) Textile

Many researchers have used FRCM to support or retrofit reinforced concrete elements such as beams, columns, and slabs [32, 33]. The textile comes in a wide range of fibers and configurations [23, 25]. The current study utilized a well-known type of textile, carbon-based Fabric-Reinforced Cementitious Matrix (Carbon-textile) system, as an external reinforcement. The characteristics of the selected textile grid include 20 mm spacing and 0.047 mm equivalent thickness. The carbon textiles' modulus of elasticity and tensile strength were 230 GPa and 3600 MPa, respectively. The carbon characteristics of the textile have been presented in Fig.1 and Table 2.

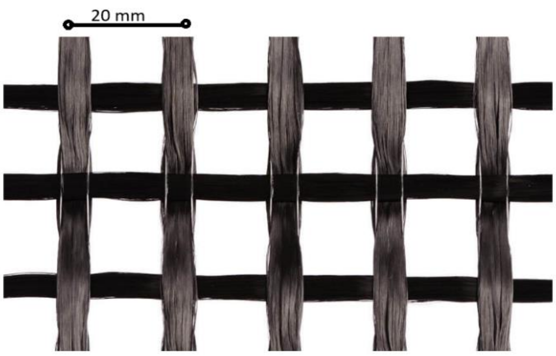

Fig. 1. Selected Carbon-textile

Table 2. Characteristics of FRCM textile based on the manufacturer's data sheet

Material	Nominal thickness	Tensile strength	Modulus of elasticity
Carbon	0.047 mm	3600 MPa	230 GPa

2.1.3 Reinforced Concrete

In the current study, the concrete slabs were cast simultaneously using ready-mix concrete. Compression testing was carried out using a calibrated testing machine, and the load was applied axially with a constant loading rate until failure occurred. The overall average compressive strength of the specimens was 34.8 MPa. The test procedure followed BS 1881: Part 116 [34].

In this experimental program, 6 mm deformed steel bars were used. The steel was tested in accordance with the requirements of the American Standard Specification for Carbon Steel Rebars for Use in Reinforced Concrete (ASTM A615/A615M-20 [35]. The diameter was measured using a micrometer, and tensile testing was performed to determine yield strength, ultimate tensile strength, and relative elongation at break. During the tensile tests, the reinforcement exhibited a well-defined linear elastic phase, followed by a distinct yield plateau and a subsequent strain-hardening region prior to rupture. The steel used is Grade 40, a type commonly used in light—and medium-duty structural applications. Table 3 shows the detailed results of the mechanical tests and the physical properties of steel bars.

Table 3. Properties of reinforcement steel.

Property	Values
Nominal diameter (mm)	6
Actual diameter (mm)	5.8
Cross-sectional area (mm2)	26.4
Yield stress (MPa)	405.3
Ultimate stress (MPa)	605
Elongation (%)	17
Nominal weight (Kg/m)	0.208
Grade	G40

2.2 Test Specimens Details

2.2.1 Specimens Details and Parameters

The main aim of this experimental study is to investigate the effectiveness of using carbon-FRCM as external reinforcement on the flexural behavior of two-way RC slabs. Four laboratory-scale RC slabs with identical geometry were constructed and tested as simply supported at their perimeter (Fig. 2). As indicated in Fig. 2 (a), the slabs were of a square section with a 1000 mm side and a thickness of 80 mm. Also, the effective flexural span was 900 mm (Fig. 2(b)).

To simulate the flexure-deficient, all the samples were lightly reinforced with a reinforcement ratio of (ρ=0.28%). Fig. 2(C) shows the details of the steel reinforcement for the samples. The reinforcing steel utilized in the present study was deformed steel bars with a 6 mm diameter and a spacing of 192 mm at the bottom in two directions of the slabs. All reinforcement bars have been bent at the supports by 180 degrees to guarantee proper anchorage. Also, 6 mm bars were added at distances of 100 mm from the support in the top reinforcement to control surface cracks and improve the anchoring. This was applied to all support in the four edges of the slab. To reduce cracks resulting from twisting moments, additional reinforcement was used at the corners as shown in Fig. 2(c).

To achieve the goal of this research, two parameters, the configuration of FRCM and the existence of pre-damage, were considered. Fig. 3 and Table 4 show the configurations of the FRCM and the sample details. Four samples were designed to complete the experimental programs as follows:

- R represents the control specimen tested without strengthening (Fig. 3-a).
- C250 is a sample strengthened with two carbon textile strips in a cross configuration. Every strip was 45 mm wide, 50% of the slab's effective span in each direction (Fig. 3-b).
- C50-3 is a sample strengthened with six strips of carbon textile, three of which were in a cross configuration. Each strip had a width of 15mm, representing 50% of the slab's effective span in each direction (Fig. 3-c).

CD250 is a sample strengthened with two strips of carbon textile in a cross configuration. Every strip was 45 mm wide, 50% of the slab's effective span in each direction (Fig. 3-d). This specimen is strengthened after being pre-damaged.

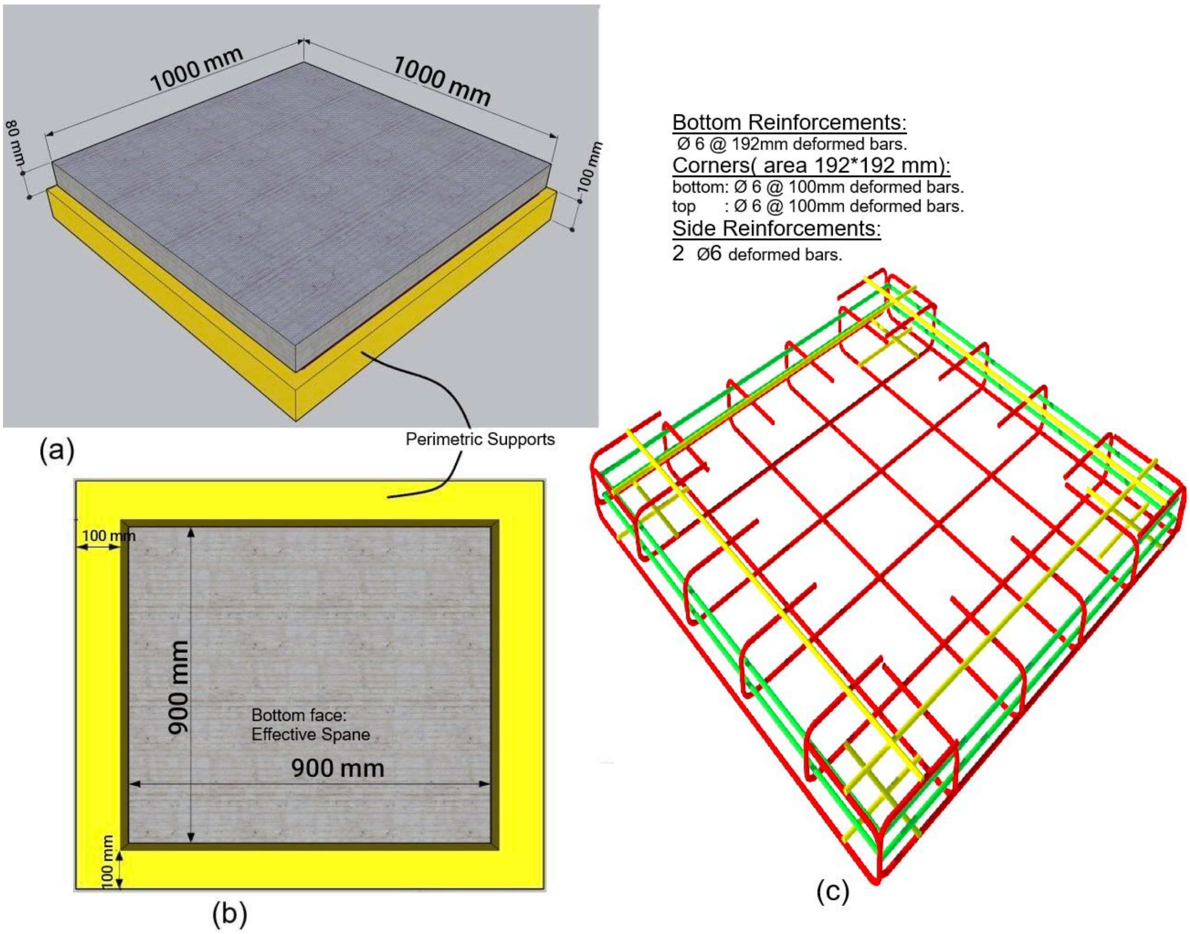

Fig. 2. (a) The slab's geometry; (b) the slab's perimeter-supported bottom face; and (c) the slab's steel reinforcement details

Table 4. Samples, experimental parameters, and materials

Samples	Strengthening configuration	Concrete compressive strength F`c (MPa)	mortar compressive strength F`mc (MPa)	steel reinforcement ratio ρs (per direction)	Textile reinforcement ratio ρt (per direction)
R		34.26		0.29%	
C250	Two carbon textile strips in a cross configuration	34.26	40	0.29%	50%
C50-3	Six carbon-textile strips, including three arranged in a cross pattern	34.26	40	0.29%	50%
CD250	Two carbon textile strips in a cross configuration	34.26	40	0.29%	50%

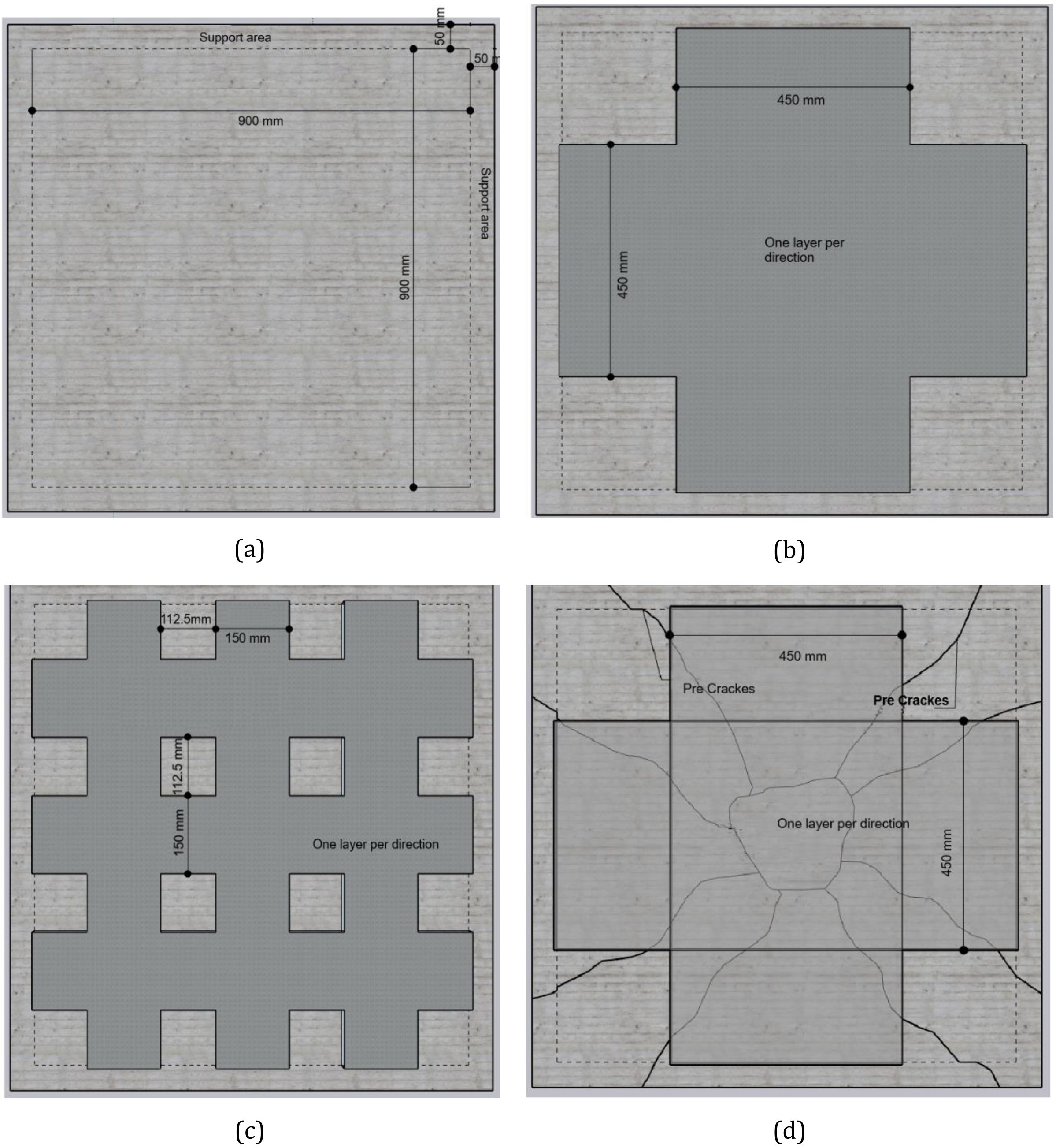

Fig. 3. Configuration of FRCM strengthening on the tested samples/ (a) Control slab R, (b) C250, (c) C50_3, and (d) CD250

2.2.2 Strengthening Procedure

In this experimental program, FRCM was adopted to retrofit the concrete slab models due to its height, tensile strength, and modulus of elasticity [23, 36]. The procedure for the application of FRCM carbon textile on the samples has been indicated in the following steps:

- Preparing concrete model surfaces by mechanical cleaning and removing dust and loose materials.
- A grid of grooves, 2mm in depth, is created to achieve good adhesion between the mortar layer and the concrete surface (Fig. 4-a).
- Moisten the concrete surface to be strengthened (Fig. 4-a).
- The first layer of cementitious mortar was applied with a thickness of 3mm at the sample's tension face on the required portion of the concrete surface according to the intended strengthening ratio (Fig. 4-b).

- The first layer of the carbon textile was applied onto the fresh cementitious mortar and gently pressed by hand to achieve full contact and adequate bonding between the fabric and the matrix (Fig. 4-b).
- The second layer of cementitious mortar was applied on the first layer of the carbon textile (Fig. 4-c).
- A new layer of the carbon textile was applied perpendicular to the previous carbon textile layer (Fig. 4-c).
- The final layer of cementitious mortar is applied, followed by careful finishing and smoothing of the surface (Fig. 4-d).

All mortar and textile layers must be applied while the mortar is still fresh.

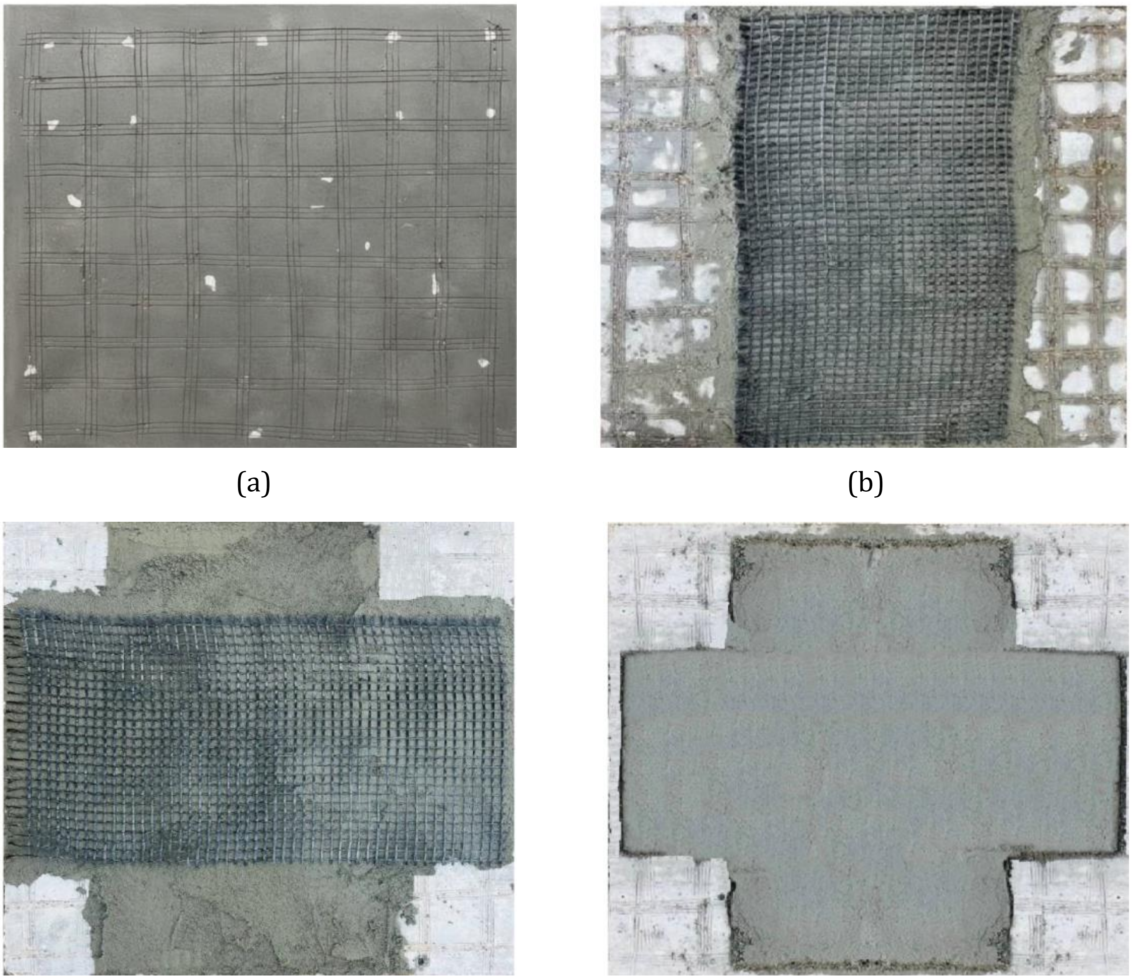

Fig. 4. Application steps for FRCM reinforcement: (a) Preparing and moistening the concrete surface for strengthening; (b) Application of the first mortar layer together with the carbon textile; (c) Application of the second mortar layer along with the carbon

2.3 Testing Set Up and Procedure

The test was performed with monotonic loading, and the entire perimeter was simply supported, as shown in Fig. 5. Four rigid steel beams were utilized as supports, which were welded with a steel bar of diameter 25mm, then a 10 cm rubber band was fixed on the top of the steel bar to ensure proper loading distribution. As illustrated in Fig. 5, the effective flexural span was 900 mm in each direction. A system of three rigid steel beams was used to disrupt the one-point load into a four-point load, as indicated in Fig. 5 (a), leading to proper load distribution. At the locations of load application, square rubber pads (100 x 100 x 10 mm) and square steel plates (100 x 100 x 12 mm) were used between the upper face of the slab and the rigid steel beams to reduce local stresses. The center-to-center distance between the four-point load was 400 mm, as indicated in Fig. 5.

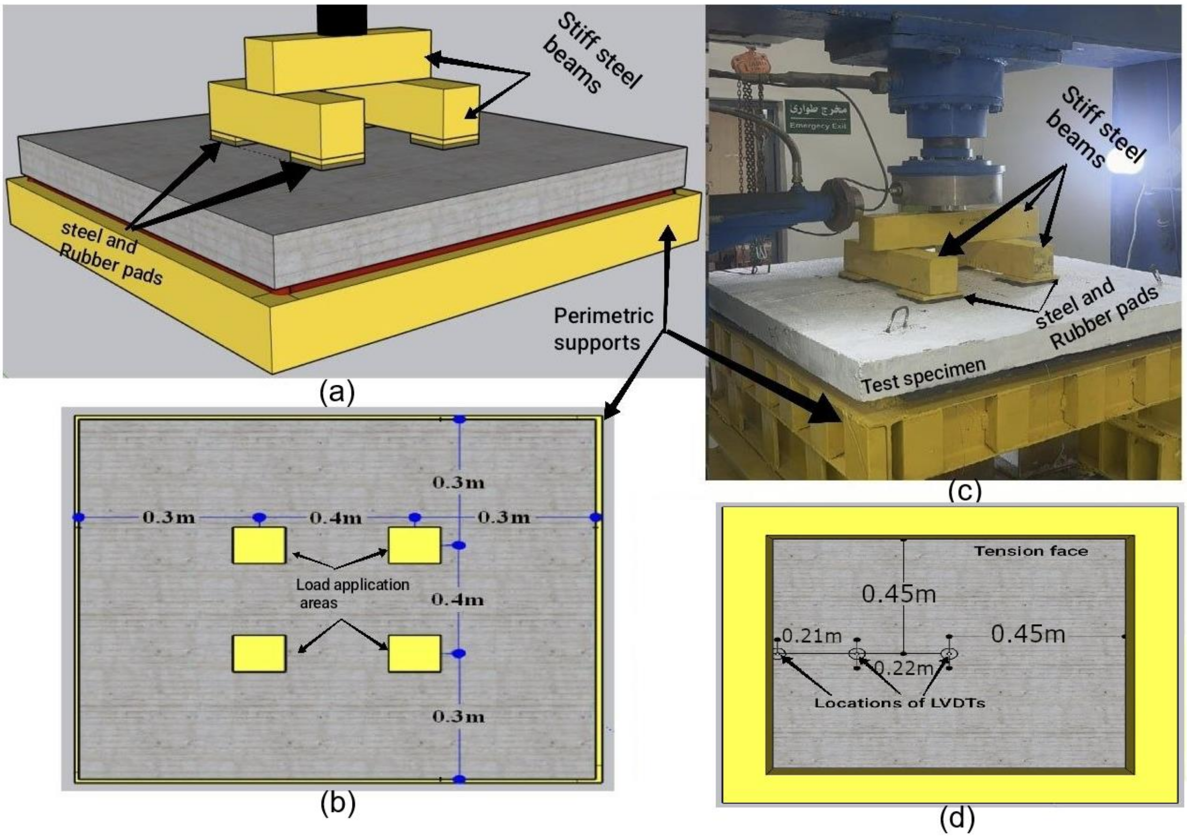

Fig. 5. Experimental setup (a) 3D schematic view; (b) top view; (c) the specimen positioning and the applied loading scheme; (d) Layout of LVDTs installed for deflection measurements.

The sample's deflection was observed by utilizing three linear variable differential transformers (LVDT), as indicated in Fig. 5 (d). Three LVDTs were installed on the slab to measure its deflection. The first one is placed at the center to record the central deflection, the second one is located in the middle between the center and the support to catch the intermediate deflection, and the third is near the support to measure the deflection at this point. All the samples have been loaded up to failure except CD250. First, it is loaded with 50% of the ultimate load, followed by the strengthening that is applied, and then, CD250 is tested up to failure.

3. Experimental Findings

The results of all tested slabs were indicated in Fig. 6 as curves illustrating the relationship between the loads and the deflection at the center of the slabs. Fig. 7 indicates the ultimate crack pattern for each sample. The main experimental results, including the ultimate load Pmax, the ultimate deflection and the improvement in the flexural strength due to the retrofitting process, have been indicated in Table 5. To provide a precise mathematical definition for the stiffness derivation, the initial pre-cracking stiffness (K_{cr}) was calculated using linear regression as the average secant slope of the load–midspan deflection curve for the uncracked stage($K = \Delta P/\Delta \delta$, form the origin up to the cracking load). The cracking load was estimated as the load level where the first crack was noticed during the test and where the slope of the load–deflection curve starts to change. Subsequently, the post-cracking stiffness (K_{post}) was mathematically derived as the average linear slope of the data points extracted from the cracking point up to the yielding stage. The load at the short-term serviceability limit state (SLS) was determined following the recommendations of Eurocode 2—Part 1 (CEN 2004)[37]. According to this standard, the SLS is reached when the midspan deflection equals L/250, where L represents the effective span of the slab. In the present study, this corresponds to a midspan deflection of about 3.6 mm. All these parameters, including this property and the ones mentioned earlier, are summarized in Table 5.

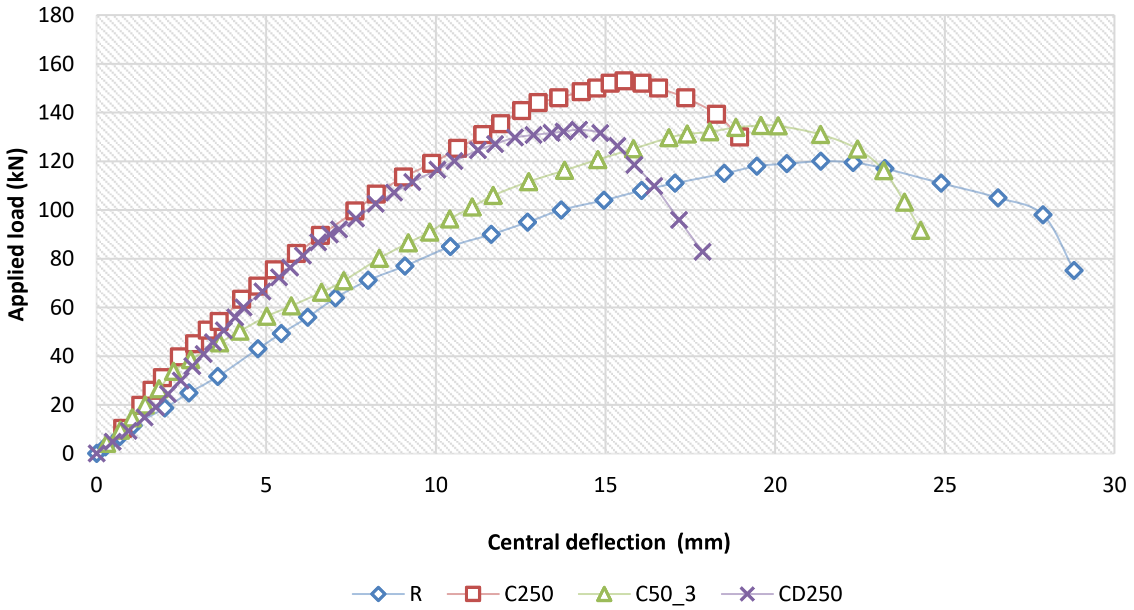

Fig. 6. Applied load versus central deflection curves for all specimens

As it was designed, the control slab (R) failed mainly in flexure after the steel bars started to yield and some large plastic deformations appeared. The first flexural cracks were seen at a load of about 15 KN, which caused a clear drop in stiffness, as can be noticed from the slope change in Fig. 6. After that, the steel reinforcement continued to yield and more cracks developed (Fig. 7(a)), together with larger deflections. Finally, the control slab reached its maximum load of around 120 KN, where many cracks appeared at the bottom face of the slab as shown in Fig. 7(a).

Sample C250, which was strengthened with two carbon textile strips in a cross configuration. Every strip was 45 mm wide, 50% of the slab's effective span in each direction. This slab showed a flexure-dominated failure mode, the same as the control slab (R), but resisted a significantly higher ultimate load of 153 KN due to the additional flexural strength provided by the FRCM layers. Additionally, it exhibits a better pre-cracking response compared to the control specimen, with a 60% increase in initial stiffness, as indicated in Table 5. Furthermore, a significant increase in the cracking load, which reached 40 KN, is illustrated in the slope of the load-deflection curve in Fig. 6. The instantaneous tensile activation of carbon fibers across flexural fractures led to a significant enhancement in post-cracking flexural stiffness, achieving 3 KN/mm, in contrast to 1.13 KN/mm for the control slab. The crack pattern of slab C250, as shown in Fig. 7(b), consisted of a few main cracks, along with some smaller ones that spread across the FRCM surface. The failure occurred gradually, primarily because some of the fibers began to slip and partially break within the mortar along the main cracks. While advanced instrumentation, such as distributed strain measurements, was not utilized to quantify the micro-mechanics of crack bridging, the progressive activation of the carbon fibers and the ultimate failure mechanisms (e.g., fiber slip and partial rupture) were phenomenologically evaluated through continuous visual monitoring of the crack development and the global load-deflection responses. Furthermore, while this qualitative assessment of crack propagation does not provide a numerical estimation of fracture energy or progressive damage modeling, it offers essential physical evidence regarding the effectiveness of the carbon textile in distributing stresses and altering the failure mechanism.

Slab C50-3, which had the same amount of textile reinforcement as slab C250 but arranged in a slightly different way (Fig. 7(c)), failed under an ultimate load of 135 KN in flexure. Its initial stiffness was even higher than specimen R, reaching roughly 16.6 KN/mm. The first visible cracks formed when the load got to around 35 KN, and the post-cracking stiffness of this slab was about 2.36 kN/mm, which is noticeably lower than that of C250 (3 kN/mm) but higher than the control slab R (1.13 kN/mm). This indicates that the material performed well compared to R; however, at this stage, placing the FRCM in the regions of maximum moments would be more effective than distributing it in strips, as was done in this specimen.

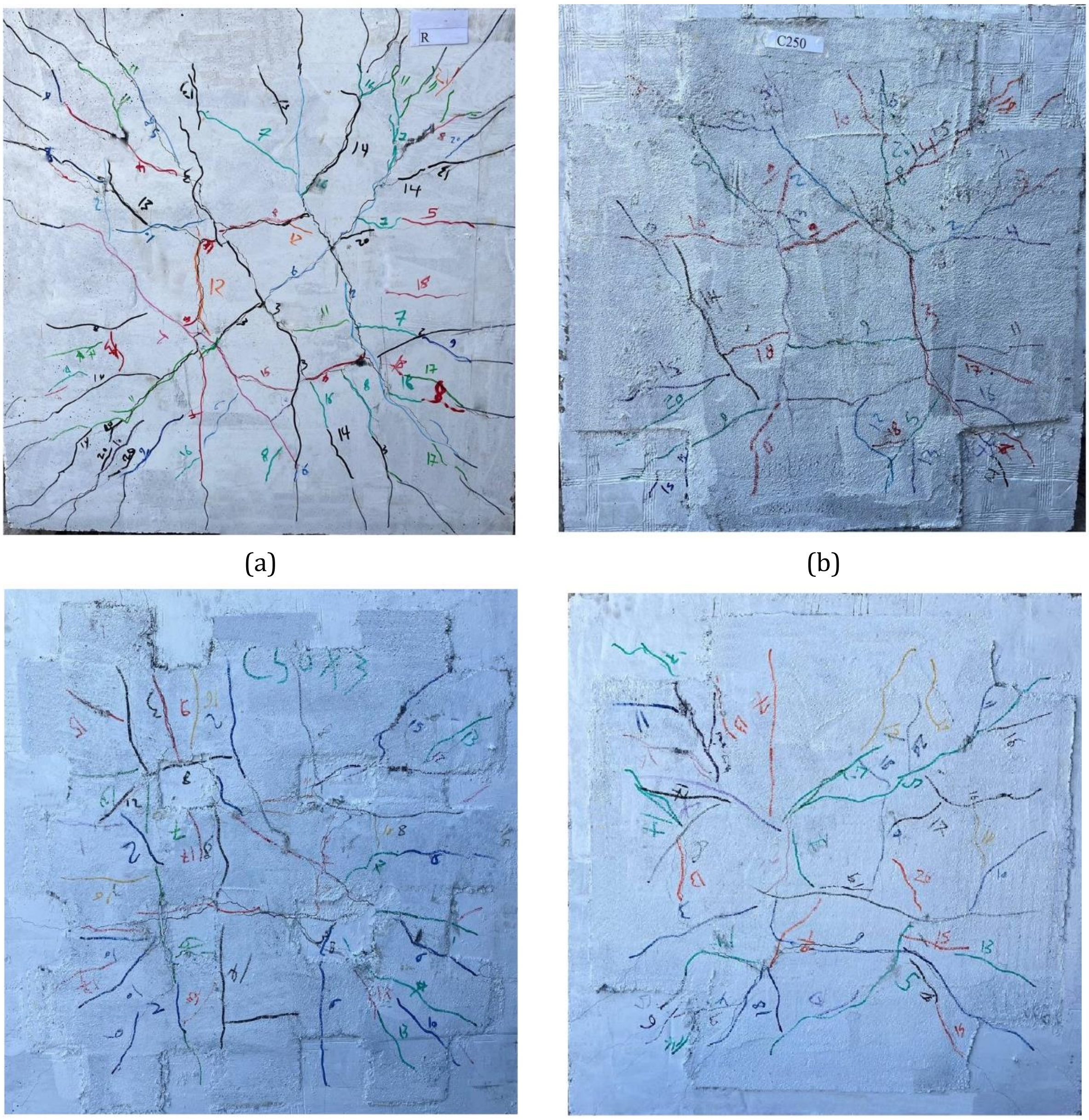

(a) (b) (c) (d)

Fig. 7. Comparison of experimental crack propagation and failure modes for the tested specimens: (a) Control slab R; (b) Strengthened slab C250; (c) Strengthened slab C50_3; (d) pre-damaged strengthened slab CD250

Table 5. Overview of the test results

Sample	Maximum load Pmax (kN)	Midspan deflection at Pmax (mm)	Improvement in capacity (%)	Pre-cracking stiffness [a] (kN/mm)	Cracking load level [b] (kN)	Post-cracking stiffness [a] (kN/mm)	Load at services (kN)
R	120.0	21.3	--------	10.6	15	1.13	31
C250	153.0	15.5	27.5	17.1(60%)	40	3 (165%)	55(77%)
C50_3	134.5	19.5	12.5	16.6(56%)	35	2.3(108%)	45(45%)
CD250	132.9	14.2	10.0	-----------	---------	1.60(41%)	

[a] *For the retrofitted specimens, the percentage increase with respect to the R specimen is provided in parentheses.*
[b] *Based on (a) the load-displacement curve's slope change and (b) the test results.*

The specimen finally failed in flexure after the steel bars yielded and the textile fibers started slipping inside the mortar, with a maximum failure load of 134.5 kN. Specimen CD250, which was pre-damaged and then strengthened with the same strengthening as specimen C250 before the test, failed in flexure under a load of about 132.9 KN. This specimen showed a lower initial stiffness compared with the other samples, mainly because of the pre-cracking of concrete as indicated in Fig. 7. At a load of 50 KN, the FRCM reinforcing layers start contributing to resisting the tension stresses, where the stiffness increases significantly.

4. Discussion and Evaluation of the Findings

The strengthening methods employed in this study successfully provided a noticeable improvement in the flexural strength of the lightly-reinforced concrete two-way slabs. From an analytical perspective, the carbon textile enhances the flexural capacity by contributing to the internal tensile force equilibrium after concrete cracking, thereby delaying the yielding of the internal steel. However, evaluating this capacity theoretically requires complex sectional equilibrium analysis combined with spatial failure mechanisms. Predicting the exact ultimate load is highly challenging due to the progressive nature of fiber-matrix debonding and the discrete distribution of the strengthening strips. Consequently, while developing a rigorous analytical and numerical model to validate these capacities is a primary objective for our future ongoing research, the current study intentionally focuses on establishing a solid physical baseline through experimental macroscopic evaluation. Considering the different variables examined, a review of the experimental results presented in Table 5 including the ultimate strength, cracking load, pre-cracking stiffness, post-cracking stiffness, and the response at the serviceability limit state (SLS) points out several key observations and outcomes that are discussed below.

4.1 Effect of Fiber-Reinforced Cementitious Mortar Layers

In general, the FRCM layer achieves a significant increase in flexural strength, which is consistent with the findings of several studies, which state that the textile-reinforced systems provide additional tensile resistance to concrete elements This improvement is mostly due to the fact that the carbon fibers start working early on during loading. This makes it easier for tensile stresses to spread evenly over the concrete–mortar–textile composite layers.

In addition to the higher ultimate load, the strengthened slabs also exhibited a higher initial stiffness just before cracking, indicating that a more stable response and a proper interaction bond between the slab and the FRCM were functioning effectively. Even after the cracking initiated, the slabs still exhibited higher degrees of post-cracking stiffness, largely due to the carbon fibers maintaining the cracks and delaying their opening. This behavior is very similar to what other researchers mentioned before, where FRCM systems usually help with crack control and keeping the stiffness from dropping too much after cracking [38].

Also, the service-load behavior improved in all strengthened slabs, not just in terms of strength but also in how the slabs behaved under normal loading levels, which is really important for long-term use. Furthermore, regarding long-term environmental durability, the inorganic nature of the cementitious matrix offers inherent advantages over traditional resin-based FRP systems. It provides excellent thermal compatibility with the concrete substrate, superior resistance to ultraviolet (UV) radiation, and allows moisture breathability, thereby reducing the risk of premature delamination and ensuring sustained structural performance over time. These trends can be seen in the load–deflection curves in Fig. 6, and the values listed in Table 5 also support the idea that the FRCM strengthening method had a positive effect on the performance of the two-way slabs used in this study.

4.2 Configuration FRCM layer

An insight into the effect of the strengthening configuration is provided in specimens C250 and C50_3, whose test results are retrievable in the summary format of Table 5 and also in the plots of Fig. 3. Despite using the same type of carbon FRCM and having the same reinforcement ratio (two orthogonal textile layers covering nearly 50 per cent of the tension face), the arrangement of these layers was completely different. Specimen C250 was laid with each layer in a single sheet and placed at the center of the span where the maximum bending moment occurs. That meant that the majority of the textile was focused directly where the slab required its maximum tensile reinforcement. For C50_3, on the other hand, each of the layers was separated into three strips of 15 cm in width spaced by roughly 11.25 cm. In this configuration, the textile can be spread over a larger volume, and its fibers may interact progressively, according to the formation and propagation of cracks. Fig. 3 clearly shows the layouts of both configurations and may help explain why the reinforcement in C250 seems to have been activated more directly and efficiently.

These differences in configurations had an obvious impact on the mechanical behavior. Specimen C250 exhibited a higher ultimate load (153 kN) than C50_3 (135 kN), indicating the superior flexural efficiency of placing the reinforcement directly in the maximum moment area (Table 5). This performance is fundamentally linked to the micro-mechanical interaction between the fiber and the matrix. In C250, the continuous mesh configuration provided a larger effective surface area for bond stress distribution, which enhanced the mechanical interlock (the "rivet effect") where the mortar effectively penetrated the grid openings. This mechanism delayed the initiation of fiber-matrix debonding and resisted its progression across the span. In contrast, the discontinuous strips in C50_3 created localized stress concentrations at the edges of each strip, leading to an earlier onset of debonding and less efficient crack bridging. This is reflected in the cracking load, which rose significantly from 15 kN in the control slab to 40 kN in C250, compared to 35 kN in C50_3. Furthermore, C250 achieved nearly double the post-cracking stiffness (3 kN/mm) compared to C50_3 (2.36 kN/mm), as the dense, centralized grid was more effective in arresting micro-crack propagation within the cementitious matrix. The behavior remained consistent for the serviceability limit state (SLS) resistance, with C250 reaching 55 kN while C50_3 reached 45 kN. Although both configurations outperformed the control specimen, the concentration of FRCM in the maximum moment region enabled fibers to bridge cracks more effectively. The distributed-strip configuration (C50_3) enhanced performance but did so by only partially engaging the fibers, as some strips were slightly off the major cracking path, further facilitating the debonding progression compared to the continuous patch in C250.

4.3 Effectiveness of FRCM Strengthening on Pre-Cracked Slabs

The effectiveness of FRCM strengthening after initial cracking was evaluated by comparing specimen CD250, which was subjected to 50% of the ultimate load of the control slab before strengthening, with the directly strengthened specimen C250. Both specimens utilized the same carbon FRCM with two orthogonal layers covering 50% of the tension face, and their layout is illustrated in Fig. 3. In CD250, flexural cracks had already developed prior to the application of FRCM, whereas C250 was strengthened without any prior damage. The pre-existing cracks in CD250 were flexural in nature. Despite this initial damage, the slab was able to achieve a final load capacity of 132.9 KN, which is significantly higher than the control slab (120 KN) but still lower than C250 (153 KN). CD250 achieved a post–cracking stiffness of 1.6 KN/mm, which is only 41% larger than for the control slab (1.13 KN/mm) but 68% less than for C250 (3 KN/mm). As summarized in Table 5 and plotted in Fig. 6, these results demonstrate that FRCM can regain some of the lost flexural capacity and stiffness. However, this is depreciated when compared with undamaged slabs that were subsequently strengthened.

Despite these small differences, CD250 performed similarly to C250 in failure mode (no or minimally debonded and slipped fiber), and there were no significant issues (dis-) activating FRCM during loading. While the extremely slight, probably negligible, effect of pre-existing cracks slightly impaired textile layer engagement (lowering the post-cracking stiffness in them compared to a fully intact slab) and contributed slightly to the detection of cracks, it could not prevent effective crack bridging and net flexural reinforcement. Relative to the control slab, CD250 showed a significant increase in ultimate capacity and post-cracking behavior, demonstrating that FRCM can even be effective if the damage is applied first. In conclusion, FRCM has proven to be efficient in increasing flexural performance compared to direct strengthening (C250), providing additional (up to 27%) structural compensation and controlling the crack texture even when bonded after moderate pre-damage. The differences are highlighted by the position of reinforcement with respect to the region of maximum moment (Fig. 6) and the need for optimized behavior between different structural systems.

Despite the slight differences, the failure mode of CD250 remained similar to C250, with no significant issues in fiber debonding or slippage, although minor differences in FRCM activation during loading were observed. The presence of pre-existing cracks slightly affected the engagement of the textile layers, reducing the post-cracking stiffness compared to the fully intact slab, but did not prevent effective crack bridging and flexural reinforcement. Compared with the control slab, CD250 exhibited a substantial enhancement in both ultimate capacity and post-cracking response, confirming that FRCM can be effective even when applied after initial cracking. Overall, the comparison highlights that while direct strengthening (C250) yields the highest flexural performance, applying FRCM after moderate pre-damage still provides meaningful structural improvements, particularly in load-bearing capacity and crack control. The observed differences underline the importance of reinforcement placement relative to the maximum moment region, as shown in Fig. 6, in achieving optimal structural performance.

5. Conclusion

The present research paper provides experimental insights into the effectiveness of the carbon-roving FRCM system in enhancing the behavior of two-way RC slabs, when applied to strengthen undamaged members and to repair pre-damaged ones. The research was focused on different performance parameters, including ultimate flexural strength, first-crack load, pre-crack and post-crack stiffness development, crack pattern and propagation, and service load behavior of the slabs. Using these criteria, the key findings from the experimental program can be summarized as follows:

- The FRCM was efficient in retrofitting RC slabs, as all retrofitted slabs showed a significant difference from the control slab in various scales.
- The distribution of FRCM layers under the loaded areas should be placed just above the maximum moment zone rather than distributing them as separate strips. The slabs with such layers presented significant improvements in terms of the failure load, stiffness, and crack control.
- FRCM usage demonstrates high effectiveness in increasing the first cracking loading, resulting in more elastic and stable behavior.
- An overall enhancement in structural stiffness was observed in both the pre-cracking and post-cracking stages, particularly in the specimens strengthened with continuous textile reinforcement. This indicates a more effective engagement of the textile in resisting deformation throughout the entire loading process.
- More effective crack control is achieved with the reinforcement in the critical zone. The strip layout still helped, but somewhat imperfectly because the strips are not contiguous.
- Strengthened slabs have a higher load-to-allowable deflection ratio, which enhances the serviceability behavior of the slabs.
- The outcome showed not only that the amount of surface covered is significant, but also the design and configuration of the fibers.

Based on the above, future studies are recommended to evaluate different coverage ratios, better spacing for strip layouts, other types of textile materials, and also the long-term behavior of FRCM under repeated loads and different environmental conditions. These aspects could help in developing more reliable and efficient strengthening strategies for using FRCM in real repair and retrofitting projects.

References

[1] Sahranavard S, Jahangir H, Kazemi HH. An experimental and numerical investigation of RC slabs externally strengthened by perforated steel plates. In: Structures. Elsevier; 2022. https://doi.org/10.1016/j.istruc.2022.09.030

[2] Kadhim EM, Altaie MR. Factors Affecting Maintenance Practises in Iraq's Hospital Buildings. Jordan Journal of Civil Engineering. 2023;17(3). https://doi.org/10.14525/JJCE.v17i3.04

[3] Harith IK, et al. Prediction of high-performance concrete strength using machine learning with hierarchical regression. Multiscale and Multidisciplinary Modeling, Experiments and Design. 2024;7(5):4911-4922. https://doi.org/10.1007/s41939-024-00467-7
[4] Chmielewski R, Baryłka A, Obolewicz J. Analysis of design solutions for strengthening the load-bearing structure of a building for further safe use. Journal of Achievements in Materials and Manufacturing Engineering. 2021;104(1). https://doi.org/10.5604/01.3001.0014.8481
[5] Mai A D, Lee C K, Nguyen C L. Flexural performance of composite beam with high-strength steel girder and ECC slab: A comprehensive parametric study. Res. Eng. Struct. Mater., 2025; 11(3): 1345-1367. http://dx.doi.org/10.17515/resm2025-860ma0502rs
[6] Aykac S, Kalkan I, Tankut T. Flexural strengthening and repair of RC slabs by adding a new RC layer. Structural Concrete. 2016;17(5):896-909. https://doi.org/10.1002/suco.201500182
[7] Aldhafairi F, et al. Different techniques of steel jacketing for retrofitting of different types of concrete beams after elevated temperature exposure. In: Structures. Elsevier; 2020. https://doi.org/10.1016/j.istruc.2020.09.017
[8] Jumaat MZ, Alam MA. Problems associated with plate bonding methods of strengthening reinforced concrete beams. Journal of Applied Sciences Research. 2006;2(10):703-708.
[9] Alam MA, Al-Amin M. Anchors for shear strengthening of damaged RC beam using bonded steel plate. Res. Eng. Struct. Mater., 2023; 9(4): 1361-1377. http://dx.doi.org/10.17515/resm2023.678st0130
[10] Hamzah MK, Rashid RSM, Hejazi F. Cyclic performance of exterior RC beam-column strengthened with different thicknesses of CFRP sheets. In: IOP Conference Series: Earth and Environmental Science. IOP Publishing; 2022. https://doi.org/10.1088/1755-1315/961/1/012069
[11] Abbas MK, Hamzah MK. Numerical investigation on flexural performance of hybrid concrete T-beams. In: AIP Conference Proceedings. AIP Publishing LLC; 2023. https://doi.org/10.1063/5.0166265
[12] Siddika A, et al. Strengthening of reinforced concrete beams by using fiber-reinforced polymer composites: A review. Journal of Building Engineering. 2019;25:100798. https://doi.org/10.1016/j.jobe.2019.100798
[13] Hamzah MK. Replacement of Flexural and Shear Reinforcement of Double-Column Bridge Bent with CFRP under Combined loadings. In: IOP Conference Series: Earth and Environmental Science. IOP Publishing; 2022. https://doi.org/10.1088/1755-1315/961/1/012070
[14] Fang H, et al. Flexural behavior of composite concrete slabs reinforced by FRP grid facesheets. Composites Part B: Engineering. 2016;92:46-62. https://doi.org/10.1016/j.compositesb.2016.02.029
[15] Erfan AM, et al. Flexural behavior of HSC one way slabs reinforced with basalt FRP bars. Case Studies in Construction Materials. 2021;14:e00513. https://doi.org/10.1016/j.cscm.2021.e00513
[16] He W, et al. Efficiency of different BFRP-based strengthening techniques in improving flexural behavior of RC slabs. Construction and Building Materials. 2021;308:125002. https://doi.org/10.1016/j.conbuildmat.2021.125002
[17] Arora S, et al. A review of fatigue behavior of FRP composites. Materials Today: Proceedings. 2022;64:1272-1275. https://doi.org/10.1016/j.matpr.2022.04.034
[18] Harle SM. Durability and long-term performance of fiber reinforced polymer (FRP) composites: A review. In: Structures. Elsevier; 2024. https://doi.org/10.1016/j.istruc.2024.105881
[19] Bazli M, et al. Effects of UV radiation, moisture and elevated temperature on mechanical properties of GFRP pultruded profiles. Construction and Building Materials. 2020;231:117137. https://doi.org/10.1016/j.conbuildmat.2019.117137
[20] Zhang C, Li Y, Wu J. Mechanical properties of fiber-reinforced polymer (FRP) composites at elevated temperatures. Buildings. 2023;13(1):67. https://doi.org/10.3390/buildings13010067
[21] Donnini J, Corinaldesi V. Mechanical characterization of different FRCM systems for structural reinforcement. Construction and Building Materials. 2017;145:565-575. https://doi.org/10.1016/j.conbuildmat.2017.04.051
[22] Adheem AH, et al. Confinement model for concrete wrapped with fiber reinforced cementitious mortar. Construction and Building Materials. 2021;312:125401. https://doi.org/10.1016/j.conbuildmat.2021.125401
[23] Kadhim MM, et al. Analysis and design of two-way slabs strengthened in flexure with FRCM. Engineering Structures. 2022;256:113983. https://doi.org/10.1016/j.engstruct.2022.113983
[24] Consiglio Superiore dei Lavori Pubblici (CSLP). Linee Guida per la Progettazione, l'Esecuzione ed il Controllo di Interventi di Consolidamento Statico mediante l'utilizzo di Compositi Fibrorinforzati. 2018.
[25] Ma P, Yuan S, Jia S. Bond Behavior Between Fabric-Reinforced Cementitious Matrix (FRCM) Composites and Different Substrates: An Experimental Investigation. Journal of Composites Science. 2025;9(8):407. https://doi.org/10.3390/jcs9080407
[26] Varma DA, et al. Performance Comparison of Fiber Reinforced Polymer (FRP) systems and Textile Reinforced Mortar (TRM) for Concrete Confinement at Elevated Temperature. Composites Part C: Open Access. 2025:100628. https://doi.org/10.1016/j.jcomc.2025.100628

[27] Hasan HH, Georgescu P. Concrete Columns Strengthened with Fiber Reinforced Cementitious Matrix (FRCM). Modelling in Civil Environmental Engineering. 2021;16(2):34-44.
[28] Fagone M, et al. The Bond Behaviour of FRP and FRCM Strengthening Sheets Externally Bonded to Masonry Pillars: An Experimental Based Comparison. In: International Conference of Steel and Composite for Engineering Structures. Springer; 2023. https://doi.org/10.1007/978-3-031-57224-1_8
[29] Ferretti F, Canestri M, Mazzotti C. Effect of temperature variations on the bond behavior of FRCM applied to masonry. Materials and Structures. 2022;55(6):166. https://doi.org/10.1617/s11527-022-02002-x
[30] Sagare SS, Kirthiga R, Elavenil S. A state of art of review on strengthening of concrete structures using fabric reinforced cementitious matrix. Research on Engineering Structures and Materials. 2024;10:1231-1260. https://doi.org/10.17515/resm2024.133ma1226rv
[31] Flores Ferreira K, et al. Experimental investigation on the use of Fabric-Reinforced Cementitious Mortars for the retrofitting of reinforced concrete dapped-end beams. Structural Concrete. 2023;24(4):4577-4605. https://doi.org/10.1002/suco.202200743
[32] Daneshvar K, et al. Enhancing flexural and shear capacities of RC T-beams with FRCM incorporating a full FRCM-concrete bond. Construction and Building Materials. 2025;471:140687. https://doi.org/10.1016/j.conbuildmat.2025.140687
[33] Raza A, et al. Rapid repair of geopolymer concrete members reinforced with polymer composites: Parametric study and analytical modeling. Engineering Structures. 2024;299:117143. https://doi.org/10.1016/j.engstruct.2023.117143
[34] British Standards Institution (BSI). BS 1881-116: Testing concrete - Part 116: Method for determination of compressive strength of concrete cubes. London: BSI; 1983.
[35] ASTM International. ASTM A615/A615M-20: Standard Specification for Deformed and Plain Carbon-Steel Bars for Concrete Reinforcement. West Conshohocken, PA: ASTM International; 2020.
[36] Al-Lami K, D'Antino T, Colombi P. Durability of fabric-reinforced cementitious matrix (FRCM) composites: A review. Applied Sciences. 2020;10(5):1714. https://doi.org/10.3390/app10051714
[37] European Committee for Standardization (CEN). EN 1992-1-1:2004 Eurocode 2: Design of concrete structures - Part 1-1: General rules and rules for buildings. Brussels: CEN; 2004.
[38] Abutahnat Y, Sorelli L, El Refai A. Tensile behavior of fiber-reinforced cementitious matrix with ultra-high-performance hybrid fiber-reinforced concrete (UHP-FRCM) with enhanced crack width control, fracture energy, and ultimate strength. Construction and Building Materials. 2025;489:142430. https://doi.org/10.1016/j.conbuildmat.2025.142430